FFEMS Fatigue & Fracture of Engineering Materials & Structures
ORIGINAL CONTRIBUTION
doi: 10.1111/ffe.12374

Generalized approach to estimation of strains and stresses at blunt V-notches under non-localized creep

P. GALLO[1], F. BERTO[1] and G. GLINKA[2]

[1]*Department of Management and Engineering, University of Padova, Stradella S. Nicola 3, 36100 Vicenza, Italy,* [2]*Department of Mechanical and Mechatronics Engineering, University of Waterloo, University Avenue 200, Waterloo, Ontario, Canada N2L3G1*

Received Date: 9 September 2015; Accepted Date: 3 November 2015; Published Online: 4 December 2015

ABSTRACT Geometrical discontinuities such as notches need to be carefully analysed by engineers because of the stress concentration generated by them. Notches become even more important when the component is subjected, in service, to very severe conditions, such as high-temperature fatigue and imposed viscoplastic behaviour such as creep. The knowledge of strains and stresses in such stress concentration zones is essential for an efficient and safe design process. The aim of the paper is to present an improvement and extension of the existing notch-tip creep stress–strain analysis method developed by Nuñez and Glinka, validated for U-notches only, to a wide variety of blunt V-notches. The key in obtaining the extension to blunt V-notches is the substitution of the Creager–Paris equations with the more generalized Lazzarin–Tovo solution, allowing a unified approach to the evaluation of linear elastic stress fields in the neighbourhood of both cracks and notches. Numerous examples have been analysed to date, and the stress fields obtained according to the proposed method were compared with appropriate finite element data, resulting in a very good agreement. In view of the promising results discussed in the paper, authors are considering possible further extension to sharp V-notches and cracks introducing the concept of the strain energy density.

Keywords creep; non-localized creep; stress fields; U-notches; V-notches.

NOMENCLATURE

a = notch depth
C_p = plastic zone correction factor
d = distance from the coordinate system origin at which the far-field contribution is evaluated
K_I = mode I stress intensity factor
K_t = stress concentration factor
K_Ω = strain energy concentration factor
r = radial coordinate
r_0 = distance within notch tip and coordinate system origin
r_p = plastic zone radius
t = time
2α = notch opening angle
Δr_p = plastic zone increment
Δt_n = time increment
$\Delta\varepsilon_{22}^{c_n}$ = creep strain increment at the notch tip at step n
$\Delta\varepsilon_{22}^{cf_n}$ = incremental far-field creep strain
$\Delta\varepsilon_{22}^{t_n}$ = increment of total strain
$\Delta\sigma_{22}^{t_n}$ = stress decrement at the notch tip at step n
ε_{ij}^{0} = actual elastic–plastic strain
ε_{22}^{cf} = creep strain at the far field
$\varepsilon_{22}^{c_n}$ = creep strain at the notch tip

Correspondence: F. Berto. E-mail: berto@gest.unipd.it

ε_{ij}^{e} = hypothetical strain components obtained from linear elastic analysis
ε^{p0} = plastic strain at time $t = 0$
ε_{22}^{t} = time-dependent notch-tip strain
θ = angular coordinate
ρ = notch-tip radius
σ_{ij}^{0} = actual elastic–plastic stress
σ_{ij}^{e} = hypothetical stress components obtained from the linear elastic analysis
σ_{22}^{f} = far-field stress
σ_{22}^{f0} = far-field stress, $t = 0$
σ_{max} = maximum stress at the notch tip
σ_{nom} = applied nominal stress
σ_{22}^{t} = time-dependent notch-tip stress

INTRODUCTION

Analysis and design of mechanical engineering objects means the application of acceptable engineering procedures. Such procedures are used to verify the integrity and/or functionality of the entire object and its components. Because of technological progress demanding service conditions, engineering components are becoming more complex geometry-wise including various geometrical discontinuities (e.g. notches) that generate localized high stress concentration zones.[1–4] Therefore, geometrical discontinuities in a component are regions that have to be carefully considered by the engineers. They become even more important when, in operating conditions, the component is subjected to very demanding conditions such as high-temperature fatigue.[5,6] This situation is currently very important when considering the aerospace and automotive industry.

The high-temperature environment induces time-dependent and temperature-dependent deformations resulting in a nonlinear stress–strain response such as creep (viscoplasticity). When the creep phenomena are localized or concentrated in a small region near the notch root, they can be considered as localized creep cases. However, creep strains (although low) can also occur away from the notch tip, resulting in a non-localized creep. Non-localized (or gross) creep condition refers to situations in which the far stress field also experiences some creep, and this may contribute to more intense creeping around the notch tip. This situation is not so rare in components working at high temperature. Numerous components in different applications are subjected to non-localized creep, such as power plant, gas turbine and nuclear pressure vessel industry. Gas turbine blades and disks are particularly subjected to creep phenomenon. Considering power plant, between start-up and shutdown, there is a period of on-load running. The material at the surface of the stress concentrating feature may be at constant strain during this period, and stress relaxation will take place by creep. In many other cases, pressure or centrifugal stresses may also be present, resulting in general creep deformation.[7] If these components are subjected to high temperature during constant load situation, non-localized creep must be considered.

To the best of the authors' knowledge, only a limited number of solutions concerning localized time-dependent creep-plasticity problems are available in the literature. Chaudonneret and Culie proposed an extension of Neuber's theory[8] in order to evaluate instantaneous viscoplastic notch-root behaviour under an arbitrary type of loading (i.e. creeping around notches). Several examples were presented and compared with results of numerical viscoelastic computations. However, the procedure has shown to be computationally intense. Kubo and Ohji[9] extended the concept of small-scale creep to notch problems, to develop a method for predicting the stress and strain behaviour at notches under plane-strain axisymmetric conditions. It must be underlined that, in spite of good results obtained, their method was limited to strictly localized creep, neglecting the creep effect far from the notch tip. In the work of Moftakhar *et al.*,[10] another method for predicting localized time-dependent creep stresses and strains was presented. That method was based on strain energy density considerations: it was assumed that under steady load the total strain energy density at the notch tip does not change in time even if creep is taking place around the notch tip. Therefore, the strain energy density at the notch tip can be obtained from the linear elastic solution even if the creep phenomenon is in reality taking place around the notch tip. The solution method has been derived in a general form so that it may be applied to multiaxial notch-tip stress states. Creep strains at the notch tip based on the strain energy equivalence have shown good agreement when compared with appropriate finite element data. The computation time for calculating notch-tip stresses and strains in the latest case was shorter than that one required for the finite element analysis. In the work by Härkegård and Sørbø,[11] a differential form of Neuber's rule, originally proposed by Chaudonneret and Culie,[12] has been reformulated with the purpose to

analyse a generic viscoplastic notch problem. It was shown that the stress–strain history at the notch root in a viscoplastic body can be determined directly from the elastic stress–strain response, provided that far-field viscoplastic strains could be neglected. Predictions were in good agreement with results of detailed finite element analyses.

Recently, Zhu *et al.*[13] presented singular fields near sharp V-notch for power law creep material under plane-strain condition. The theoretical solution, based on the C-integral, and the iterative method were compared with numerical simulation. Under steady-state condition, the absolute singular order only depends on the creep exponent and the V-notch angle and becomes larger with the decrease of the exponent and the angle. But for the transient, the order corresponds to the time either.

Nuñez and Glinka have recently presented in one of their papers[14] a solution for non-localized creep strains and stresses at the notch root, based on the linear elastic stress state, the constitutive law and the material creep model. The method was derived by using the Neuber total strain energy density rule.[8] This approach yielded very good results when applied to U-notches ($2\alpha = 0$ and $\rho \neq 0$). The aim of the present work is to introduce an extension of the method proposed by Nuñez and Glinka[14] to blunt V-notches. The base of the extension to blunt V-notches is the substitution of the Creager–Paris equations[15] with the more general Lazzarin–Tovo equations[16] allowing a unified evaluation of linear elastic stress fields in the neighbourhood of both cracks and notches.

The new methodology extended for V-notches, preceded by a brief introduction of the original Nuñez and Glinka[14] method and Lazzarin–Tovo's equations,[16] is discussed in the succeeding sections. The new approach has been illustrated with a number of examples showing good agreement with a set validation data obtained from detailed finite element (FE) analyses. The proposed method permits a fast evaluation of the stresses and strains at notches under non-localized creeping condition, without the use of complex and time-consuming FE nonlinear analyses. The obtained stresses and strains can be used as input parameters for life prediction creep models based on local approaches.

Some comments on the extension of the method to sharp V-notches and cracks based on the average strain energy density concept, as well as on the applicability of linear elastic approaches under creeping conditions, are discussed at the end of the paper.

NUÑEZ AND GLINKA METHOD FOR EVALUATION OF STRESSES AND STRAINS UNDER NON-LOCALIZED CREEP

The method presented in the paper by Nuñez and Glinka[14] is based on the Neuber[8] concept, and it was applied to stress–strain analysis of notched bodies with U-notches experiencing non-localized creep deformation. As stated in the introduction, the non-localized creep condition refers to a situation in which the creep takes place not only locally around the notch tip, but the far field is experiencing some creep as well. This phenomenon can be interpreted as an additional amount of energy to be added at the notch tip because of the constraint loss imposed. It will be discussed in detail later in this section. This contribution representing the non-localized effect is introduced into the original Neuber's rule for time-dependent problems.

In general, the extension of Neuber's rule to time-dependent plane stress problems can be summarized as follows:

$$\Omega = \sigma_{22}^{e}\varepsilon_{22}^{e} = \sigma_{22}^{0}\varepsilon_{22}^{0} = \sigma_{22}^{t}\varepsilon_{22}^{t} \tag{1}$$

where σ_{ij}^{e} are the hypothetical stress components obtained from the linear elastic analysis and ε_{ij}^{e} are the corresponding elastic strain components, σ_{ij}^{0} and ε_{ij}^{0} are the actual elastic–plastic stress and strain components and σ_{22}^{t} and ε_{22}^{t} are the respective time-dependent notch-tip stress and strain components. Equation (1) holds when inelastic deformations occur locally, including creep relaxation. This is due to the invariance of the total strain energy density at the notch tip ($\Omega = \sigma_{ij}^{e}\varepsilon_{ij}^{e}$) discussed by Moftakhar *et al.*[10]

In case of non-localized creep, far-field creep contribution has to be considered and Eq. (1) assumed the following form:

$$\sigma_{22}^{0}\varepsilon_{22}^{0} + K_{\Omega}\sigma_{22}^{f}\varepsilon_{22}^{cf} = \sigma_{22}^{t}\varepsilon_{22}^{t} \tag{2}$$

where $\sigma_{22}^{f}\varepsilon_{22}^{cf}$ represents the total strain energy density due to local and far-field creep.

The far-field stress in the case of a body subjected to pure axial load is assumed to be equal to the elastic stress found at a distance of three times the notch radius. In the case of pure bending load, instead, the far-field stress is defined as one-half of the nominal simple bending stress. The distance from the coordinate system origin at which the far-field contribution is evaluated is called d.

The K_{Ω} parameter[10] is the strain energy concentration factor defined as the ratio of the total strain energy density at the notch tip obtained from the linear elastic analysis to the total strain energy density at the distance d in the far field, also obtained from the linear elastic solution. This parameter takes into account the energy contribution at the notch tip due to the gross creeping condition. In fact, as briefly mentioned at the beginning of the present section, the non-localized creep can be

interpreted as an additional amount of energy to be added at the notch tip, because of the constraint loss imposed. It can be assumed that the total strain energy density changes occurring in the far field produce identical but magnified effects at the notch tip. For this reason, the total strain energy density concentration factor is introduced in order to magnify in the appropriate way the energy at the notch tip. The introduction of this parameter and of the far-field stress and strain contribution in Neuber's time-dependent formulation is the main difference within the non-localized and localized creep formulations, which, instead, can be easily derived directly by extending Neuber's rule.[14]

Because of the complexity of differential equations derived analytically for the notch stress–strain creep problem, Moftakhar *et al.*[10] proposed a special time integration method necessary for obtaining the numerical solution, namely the integration time period was divided into a finite number of discrete steps, Δt_n, and then solutions were generated for subsequent time steps. Such an approach resulted in a set of equations formulated in incremental form. The set of equations to be solved for each increment are as follows:[14]

- The creep strain increment at the notch tip at step n:

$$\Delta\varepsilon_{22}^{c_n} = \Delta t_n \cdot \dot{\varepsilon}_{22}^{c}(\sigma;t) \tag{3}$$

This is the incremental form of the creep law used in the proposed procedure, where $\dot{\varepsilon}_{22}^{c}(\sigma;t) = A\sigma^{\alpha}t^{\beta}$ is the Norton creep power law.[17]

- The stress decrement at the notch tip occurred because of the creep at step n:

$$\Delta\sigma_{22}^{t_n} = \frac{(K_\Omega C_p)\sigma_{22}^{f0}\Delta\varepsilon_{22}^{cf_n} - \sigma_{22}^{t_{n-1}}\Delta\varepsilon_{22}^{c_n}}{\frac{2}{E}\sigma_{22}^{t_{n-1}} + \varepsilon^{p0} + \varepsilon_{22}^{c_n}} \tag{4}$$

with the introduction of the Glinka plastic zone correction factor C_p.[18] The correction factor C_p is a function of the plastic zone size r_p and the plastic zone increment Δr_p. It compensates for the stress redistribution occurring at the notch tip because of the plastic yielding; K_Ω is the strain energy concentration factor[10] discussed previously; σ_{22}^{f0} is the far-field stress at the time $t=0$ (assumed to be constant during the hold time); $\sigma_{22}^{t_{n-1}}$ is the stress at the notch tip at time t for step $n-1$; $\Delta\varepsilon_{22}^{cf_n}$ is the incremental far-field creep strain while ε^{p0} and $\varepsilon_{22}^{c_n}$ are the plastic strains at time $t=0$ and the creep strain at the notch tip at step n, respectively. It must be underlined that the time-depending strain can be considered as the composition of the elastic, initial plastic and the creep strain contribution. In the last equation, the effect of the non-localized creep becomes evident and is represented by the contribution of the far field in terms of $(K_\Omega C_p)\sigma_{22}^{f0}\Delta\varepsilon_{22}^{cf_n}$. Neglecting this term, one obtains the localized creep formulation.

- Increment of the total strain:

$$\Delta\varepsilon_{22}^{t_n} = \Delta\varepsilon_{22}^{c_n} - \frac{\Delta\sigma_{22}^{t_n}}{E} \tag{5}$$

Defined as the difference between the creep strain increment at step n and the elastic strain (replaced by stress according to the Hooke law) at time t for step n.

The general stepwise procedure to generate the solution is as follows:

(1) Determine the notch-tip stress, σ_{22}^{e}, and strain, ε_{22}^{e}, using the linear elastic analysis.
(2) Determine the elastic–plastic stress, σ_{22}^{0}, and strain, ε_{22}^{0}, using the Neuber rule[8] or other methods (e.g. Equivalent Strain Energy Density ESED[19] and FE analysis).
(3) Begin the creep analysis by calculating the increment of creep strain, $\Delta\varepsilon_{22}^{c_n}$, from Eq. (3), for a given time increment Δt_n. The selected creep hardening rule has to be followed.
(4) Determine the decrement of stress, $\Delta\sigma_{22}^{t_n}$, from Eq. (4), due to the previously determined increment of creep strain, $\Delta\varepsilon_{22}^{c_n}$.
(5) For a given time increment, Δt_n, determine from Eq. (5) the increment of the total strain at the notch tip, $\Delta\varepsilon_{22}^{t_n}$.
(6) Repeat steps from 3 to 5 over the required time period.

The method can be easily programmed and yields good results for various creep data and creep hardening models, especially for notched components under constant load. However, the method can be also extended to variable loading processes. More details concerning the theoretical formulation and the description of the solution algorithm are available in the given references.[14]

Regarding the applicability of the method, the main points are the definition of the plastic zone correction factor, C_p, that is, a function of plastic zone size r_p and plastic zone increment Δr_p. Once the Creager–Paris stress distribution is assumed,[15] for $\theta=0$ in Cartesian coordinates, we have the following:

$$\begin{Bmatrix}\sigma_x\\ \sigma_y\end{Bmatrix} = \frac{K_I}{\sqrt{2\pi r}}\begin{bmatrix}1-\frac{\rho}{2r}\\ 1+\frac{\rho}{2r}\end{bmatrix} \tag{6}$$

$$\sigma_z = 0 \quad \text{(plane stress)}$$

$$\sigma_z = \upsilon(\sigma_x+\sigma_y) \quad \text{(plane strain)}$$

The origin of the coordinate system is centred at a distance from the notch tip equal to $\rho/2$, where ρ is the notch-tip radius, as shown in Fig. 1. Imposing $r=\rho/2$, one obtains the peak stress $\sigma_{\max}$ and a good approximation of the stress concentration factor K_t:

$$\sigma_{\max} = \frac{2K_I}{\sqrt{\pi\rho}} \tag{7}$$

$$K_t = \frac{\sigma_{\max}}{\sigma_{\text{nom}}} = \frac{2K_I}{\sigma_{\text{nom}}\sqrt{\pi\rho}} \tag{8}$$

$$K_I = \frac{K_t\sigma_{\text{nom}}\sqrt{\pi\rho}}{2} \tag{9}$$

Substituting Eq. (9) into Eq. (6), one obtains the stress distribution as a function of the stress concentration factor K_t and the notch-tip radius ρ:

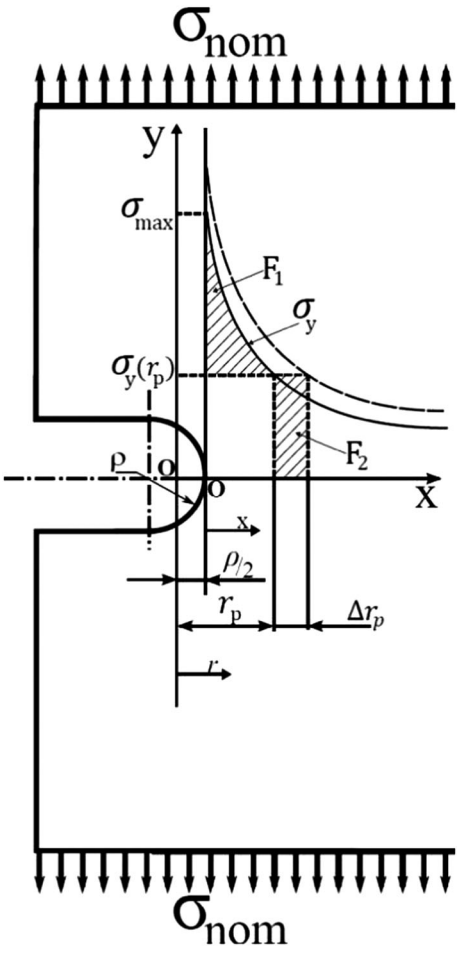

Fig. 1 Coordinate system and symbols used for the elastic stress field redistribution for U-shaped notches.

$$\begin{Bmatrix}\sigma_x\\ \sigma_y\end{Bmatrix} = \frac{K_t\sigma_{\text{nom}}}{2\sqrt{2}}\begin{bmatrix}\left(\frac{\rho}{r}\right)^{\frac{1}{2}} & -\frac{1}{2}\left(\frac{\rho}{r}\right)^{\frac{3}{2}}\\ \left(\frac{\rho}{r}\right)^{\frac{1}{2}} & +\frac{1}{2}\left(\frac{\rho}{r}\right)^{\frac{3}{2}}\end{bmatrix} \tag{10}$$

It is suggested to use a stress concentration factor K_t obtained independently from Eq. (8), in order to improve the solution of Eq. (10).

Referring to Fig. 1, considering the Mises yield criterion,[20] that is,

$$\sigma_{ys} = \sqrt{\sigma_x^2 - \sigma_x\sigma_y + \sigma_y^2} \tag{11}$$

and introducing Eq. (10) into Eq. (11), it is possible to obtain a first approximation of r_p solving numerically the following equation:

$$\sigma_{ys} = \frac{K_t\sigma_{\text{nom}}}{2\sqrt{2}}\left[\frac{\rho}{r_p} + \frac{3}{4}\left(\frac{\rho}{r_p}\right)^3\right]^{1/2} \tag{12}$$

Once r_p is known, the force F_1 (depicted in Fig. 1) can be evaluated by means of the following integral:

$$F_1 = \int_{\rho/2}^{r_p}\sigma_y \mathrm{d}r - \sigma_y(r_p)\cdot\left(r_p - \frac{1}{2}\rho\right) \tag{13}$$

where $\sigma_y(r_p)$ is the stress evaluated at a distance $r=r_p$, through Eq. (10).

Because of the plastic yielding at the notch tip, the force F_1 cannot be evaluated directly in the plastic zone defined by r_p. But in order to satisfy the equilibrium conditions, F_1 has to be carried through by the material beyond the plastic zone r_p. For this reason, stress redistribution occurs, increasing the plastic zone by the increment Δr_p.

It should be specified that the stress $\sigma_y(r_p)$ is assumed to be constant inside the plastic zone, which means elastic-perfectly plastic behaviour of the material has been assumed. Therefore, the correction factor may slightly overestimate the effect of stress redistribution.

Because $F_1 = F_2 = \sigma_y(r_p)\cdot\Delta r_p$ (all the variables are depicted in Fig. 1), the plastic zone increment Δr_p can be expressed as the ratio between F_1 and σ_y evaluated at a distance equal to the previously calculated r_p. By simple substitutions, one obtains the following explicit form of plastic increment for tension load case:[18]

$$\Delta r_p = \frac{F_1}{\sigma_y(r_p)} = \rho \frac{\left[2(r_p/\rho)^{1/2} - (\rho/r_p)^{1/2}\right]}{\left[(\rho/r_p)^{1/2} + 1/2(\rho/r_p)^{3/2}\right]} - \rho\left(\frac{r_p}{\rho} - \frac{1}{2}\right) \tag{14}$$

At last, the correction factor for the energy density C_p at the notch tip can be written as follows, for the tension load case:

$$C_p = 1 + \frac{\Delta r_p}{r_p} = 1 + \left(\frac{\rho}{r_p}\right)\left\{\frac{\left[2(r_p/\rho)^{1/2} - (\rho/r_p)^{1/2}\right]}{\left[(\rho/r_p)^{1/2} + 1/2(\rho/r_p)^{3/2}\right]} - \left(\frac{r_p}{\rho} - \frac{1}{2}\right)\right\} \tag{15}$$

It should be noted that the procedure to determine the plastic zone adjustment is analogous to that proposed by Irwin[21] for sharp notches and cracks.

More details and the bending load case are exhaustively treated by Glinka *et al.*[18]

EXTENSION OF NUÑEZ–GLINKA METHOD FOR EVALUATION OF STRESSES AND STRAINS UNDER NON-LOCALIZED CREEP TO BLUNT V-NOTCHES

The key to extend the Nuñez–Glinka method also to blunt V-notches is the introduction of the Lazzarin–Tovo equations.[16] Lazzarin and Tovo proposed in 1996 an unequivocal mathematical justified approach for notched and cracked components, with parallel or V-shaped edges. General expressions of the stress field were proposed, taking into account both the notch-tip radius and opening angle variations. It must be pointed out that the stress fields valid for sharp cracks,[22] V-cracks,[23] notch-tip radii higher than zero[15] and parallel edges[24] can be derived from the general solution, imposing approximate values to the free parameters. The Lazzarin–Tovo equations, in the presence of a traction loading, along the bisector, can be expressed as follows, as a function of the maximum stress (Fig. 2):

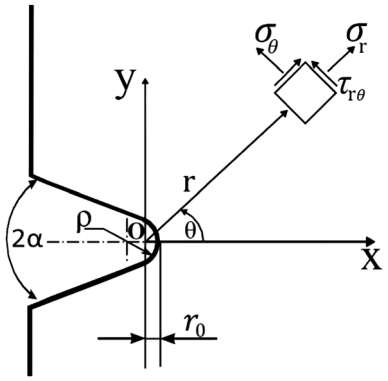

Fig. 2 Coordinate system and symbols used for the stress field components in Lazzarin–Tovo equations.

Table 1 Reference values for (mode I and mode II) power of the stress at the free surface

2α (°)	λ_1	μ_1	χ_1
0	0.5	−0.5	1
30	0.5014	−0.4057	1.0707
60	0.5122	−0.4057	1.3123
90	0.5448	−0.3449	1.8414
120	0.6157	−0.2678	3.0027
135	0.6736	−0.2198	4.1530

where $\sigma_{\max}$ can be expressed as a function of stress concentration factor K_t and the applied load σ_{nom},

$$\sigma_{\max} = K_t \sigma_{\text{nom}} \tag{17}$$

The notch radius, ρ, and the origin of the coordinate system, r_0, are related by the following equation:

$$\rho = \frac{q \cdot r_0}{q - 1} \tag{18}$$

where $q = \frac{2\pi - 2\alpha}{\pi}$.

When $q = 2$ (and so $\alpha = 0$), the origin of the coordinate system is centred at a distance $r_0 = \rho/2$ behind the notch tip, and the Lazzarin–Tovo equations immediately return the Creager–Paris equations.[15] Moreover, when $r = r_0$, one determines the stress concentration factor K_t and the elastic peak stress $\sigma_{\max}$. In Table 1, the values of the parameters introduced previously are reported for the main opening angles under mode I loading.

$$\begin{Bmatrix} \sigma_\theta \\ \sigma_r \end{Bmatrix} = \frac{\sigma_{\max}}{4}\left(\frac{r}{r_0}\right)^{\lambda_1 - 1} \begin{bmatrix} (1+\lambda_1) + \chi_1(1-\lambda_1) + \left(\frac{r}{r_0}\right)^{\mu_1 - \lambda_1}[(3-\lambda_1) - \chi_1(1-\lambda_1)] \\ (3-\lambda_1) - \chi_1(1-\lambda_1) - \left(\frac{r}{r_0}\right)^{\mu_1 - \lambda_1}[(3-\lambda_1) - \chi_1(1-\lambda_1)] \end{bmatrix} \tag{16}$$

The main steps to extend the method to blunt V-notches can be summarized as follows:

- Assumption of Lazzarin–Tovo equations to describe the stress distribution ahead the notch tip instead of Creager–Paris equations;
- Calculation of the origin of the coordinate system, r_0, as a function of the opening angle and notch radius, as described by Eq. (18);
- Redefinition of the plastic zone correction factor C_p, that is, a function of plastic zone size r_p and plastic zone increment Δr_p.

The definition of the parameters C_p, r_p and Δr_p is not so different as clearly reported by Glinka,[18] except for the assumption of different stress distribution equations. In fact, once the Lazzarin–Tovo equations are assumed, these variables are redefined automatically as briefly reported hereafter. Referring to Fig. 3, considering the Mises yield criterion[20] in polar coordinates, that is

$$\sigma_{ys} = \sqrt{\sigma_r^2 - \sigma_r\sigma_\theta + \sigma_\theta^2} \tag{19}$$

and introducing Eq. (16) into Eq. (19), it is possible to obtain a first approximation of r_p that can be solved numerically.

Once r_p is known, F_1 can be evaluated by means of the following integral:

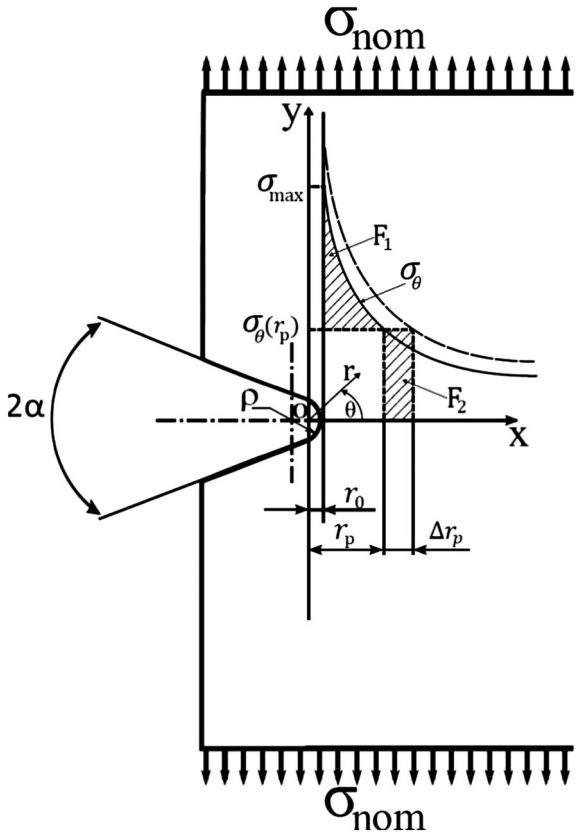

Fig. 3 Coordinate system and symbols used for the elastic stress field redistribution for blunt V-notches.

$$\begin{aligned} F_1 &= \int_{r_0}^{r_p} \sigma_\theta \mathrm{d}r - \sigma_\theta(r_p)\cdot(r_p - r_0) \\ &= \frac{K_t\sigma_{\mathrm{nom}}}{4}\left\{(r_0 - r_p)\left(\frac{r_p}{r_0}\right)^{\lambda_1-1}\left[(\lambda_1 - 1) + \chi_1(1-\lambda_1)\left[1 - \left(\frac{r_p}{r_0}\right)^{\mu_1-\lambda_1}\right] + (3-\lambda_1)\left(\frac{r_p}{r_0}\right)^{\mu_1-\lambda_1}\right]\right. \\ &\left. - \frac{[(\lambda_1+1) + \chi_1(1-\lambda_1)]\left[r_0 - r_p\left(\frac{r_p}{r_0}\right)^{\lambda_1-1}\right]}{\lambda_1} + \frac{[\chi_1(1-\lambda_1) - (3-\lambda_1)]\left[r_0 - r_p\left(\frac{r_p}{r_0}\right)^{\mu_1-1}\right]}{\mu_1}\right\} \end{aligned} \tag{20}$$

where $\sigma_\theta(r_p)$ is

$$\begin{aligned} \sigma_\theta(r_p) = \frac{K_t\sigma_{\mathrm{nom}}}{4}\left(\frac{r_p}{r_0}\right)^{\lambda_1-1}\Bigg[&(1+\lambda_1) + \chi_1(1-\lambda_1) \\ &+ \left(\frac{r_p}{r_0}\right)^{\mu_1-\lambda_1}[(3-\lambda_1) - \chi_1(1-\lambda_1)]\Bigg] \end{aligned} \tag{21}$$

The stress $\sigma_y(r_p)$ is still be considered to be constant inside the plastic zone (elastic-perfectly plastic behaviour) as commented also in the previous section. It must be underlined that, unlike what is proposed by Glinka[18], in this case, the lower integration limit is r_0, which depends on the opening angle and notch-tip radius.

As already explained in the previous section, because of the plastic yielding at the notch tip, in order to satisfy the equilibrium conditions, F_1 has to be carried through by the material beyond the plastic zone r_p, and a stress redistribution occurs, increasing the plastic zone by the increment Δr_p.

Because $F_1 = F_2 = \sigma_\theta(r_p)\cdot\Delta r_p$, the plastic zone increment can be expressed as the ratio between F_1 and σ_θ

evaluated (through Lazzarin–Tovo equations) at a distance equal to the previously calculated r_p:

$$\Delta r_p = \frac{F_1}{\sigma_\theta(r_p)} \tag{22}$$

Substituting in Eq. (22) the formula given in Eq. (20) for F_1 and the explicit form of σ_θ represented by Eq. (21), one obtains the expression for the evaluation of Δr_p:

$$\Delta r_p = \left\{ \left(\frac{r_p}{r_0}\right)^{1-\lambda_1} \left[(r_0 - r_p)\left(\frac{r_p}{r_0}\right)^{\lambda_1 - 1} \left[(\lambda_1 + 1) + \chi_1(1-\lambda_1)\left[1 - \left(\frac{r_p}{r_0}\right)^{\mu_1 - \lambda_1}\right] + (3-\lambda_1)\left(\frac{r_p}{r_0}\right)^{\mu_1 - \lambda_1}\right] \right.\right. \tag{23}$$
$$\left.\left. - \frac{[(\lambda_1 + 1) + \chi_1(1-\lambda_1)]\left[r_0 - r_p\left(\frac{r_p}{r_0}\right)^{\lambda_1 - 1}\right]}{\lambda_1} + \frac{[\chi_1(1-\lambda_1) - (3-\lambda_1)]\left[r_0 - r_p\left(\frac{r_p}{r_0}\right)^{\mu_1 - 1}\right]}{\mu_1} \right] \right\}$$
$$/\left\{ (\lambda_1 + 1) + \chi_1(1-\lambda_1)\left[1 - \left(\frac{r_p}{r_0}\right)^{\mu_1 - \lambda_1}\right] + (3-\lambda_1)\left(\frac{r_p}{r_0}\right)^{\mu_1 - \lambda_1} \right\}$$

At last, the plastic zone correction factor, C_p,[18] is defined as

$$C_p = 1 + \frac{\Delta r_p}{r_p} = 1 + \left\{ \left(\frac{r_p}{r_0}\right)^{1-\lambda_1} \left[(r_0 - r_p)\left(\frac{r_p}{r_0}\right)^{\lambda_1 - 1} \left[(\lambda_1 + 1) + \chi_1(1-\lambda_1)\left[1 - \left(\frac{r_p}{r_0}\right)^{\mu_1 - \lambda_1}\right] + (3-\lambda_1)\left(\frac{r_p}{r_0}\right)^{\mu_1 - \lambda_1}\right] \right.\right. \tag{24}$$
$$\left.\left. - \frac{[(\lambda_1 + 1) + \chi_1(1-\lambda_1)]\left[r_0 - r_p\left(\frac{r_p}{r_0}\right)^{\lambda_1 - 1}\right]}{\lambda_1} + \frac{[\chi_1(1-\lambda_1) - (3-\lambda_1)]\left[r_0 - r_p\left(\frac{r_p}{r_0}\right)^{\mu_1 - 1}\right]}{\mu_1} \right] \right\}$$
$$/\left\{ r_p\left[(\lambda_1 + 1) + \chi_1(1-\lambda_1)\left[1 - \left(\frac{r_p}{r_0}\right)^{\mu_1 - \lambda_1} + (3-\lambda_1)\left(\frac{r_p}{r_0}\right)^{\mu_1 - \lambda_1}\right]\right] \right\}$$

At this point, the general stepwise procedure to be followed to generate a solution is identical to that proposed by Nuñez and Glinka[14] and briefly reported in the previous section.

Examples of Nuñez–Glinka method applied to U-notches: considerations and comparison between numerical and finite element method analyses

The Nuñez–Glinka method has been applied to a hypothetical plate weakened by lateral symmetric U-notches, under mode I loading. The notch-tip radius ρ and the notch depth a has been varied. Three values of the notch depth, a, have been considered: 10, 15 and 20 mm. Notch-tip radius assumed for every notch depth are as follows: 0.01, 1 and 6 mm. Figure 4 depicts the considered geometry. The plate has a constant height, H, equal to 192 mm and a width, W, equal to 100 mm. The numerical results have been obtained thanks to the implementation of the method and its equations in the MATLAB® software (MathWorks, Inc., Natick, MA, USA). In order to conduct the analysis, it is necessary to define quantitatively the distance d (from the coordinate system origin) representing the 'far field' at which the elastic contribution is evaluated. Glinka *et al.*[14] proposed a value of three times the notch radius in case of a body subjected to pure axial loading. However, this solution has been found to generate good results only when the notch-tip radius is approximately bigger than 2 mm. Because for a smaller tip radius the generated d is too small, the distance at which the elastic contribution is evaluated has to be larger than three times the notch radius, in order to be in the elastic field. The correct values have been determined through a FE linear elastic analysis applying the desired load and are reported in Table 2, where d expresses the distance measured from the origin of the coordinates system, while $x(\rho)$ expresses the distance measured from the notch tip as a function of the notch radius.

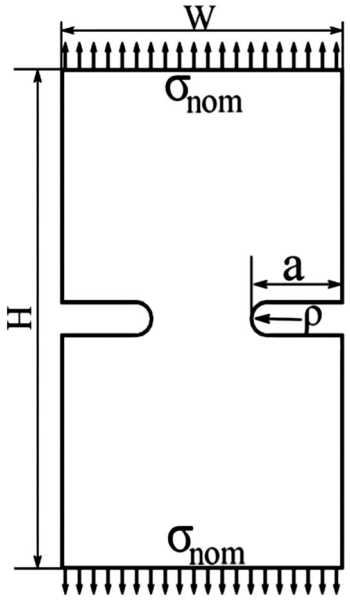

Fig. 4 Plates weakened by lateral symmetric V-notches.

Table 2 Distance d (measured from the origin of the coordinates system) at which the elastic contribution is evaluated; x is the distance from the notch tip

ρ (mm)	$x(\rho)$ (mm)	d (mm)
0.01	/	20
1	$18*\rho$	18.5
6	$3*\rho$	21

At the same time, a FE analysis has been carried out through an ANSYS code. The plate has been modelled with a Solid 8 node 183, and the plane stress condition is assumed.

The material elastic (E, v, σ_{ys}) and creep (n, B) properties are reported in Table 3. The creep law has been modelled as follows:

$$\dot{\varepsilon} = \mathrm{B} \cdot \sigma^{\mathrm{n}} \tag{25}$$

Equation (25) is very similar to that proposed by Nuñez–Glinka[14] by imposing the parameter $\beta = 0$:

Table 3 Mechanical properties

E (MPa)	v	σ_{ys} (MPa)	n	B (MPa^{-n}/h)
191 000	0.3	275.8	5	1.8

E is Young's modulus, v Poisson's ratio, σ_{ys} the yield stress and n and B the creep exponent and the creep constant, respectively.

$$\dot{\varepsilon} = A\sigma^{\alpha} t^{\beta} \tag{26}$$

A uniform load equal to 345 MPa has been applied. In order to simulate the creep relaxation, the load has been applied in different load steps: in the first one, the load has been applied instantaneously, approximately in $t = 10^{-5}$ h; subsequently, in a second load step, it has been maintained constant for the desired time t. At regular intervals during the relaxation process, the stresses and strains were stored.

The obtained results are summarized in Figs 5–7, listed as a function of the notch depth a for the sake of clarity. The results suggest a very good agreement between the numerical finite element method (FEM) values and the theoretical solution proposed in the present paper. The stresses of all of the considered geometries have been predicted correctly, also when considering the small tip radius of 0.01 mm. Furthermore, the strains present a good agreement. For the sake of brevity, the tip radius case of 0.01 mm and the strains of all of the cases are omitted here.

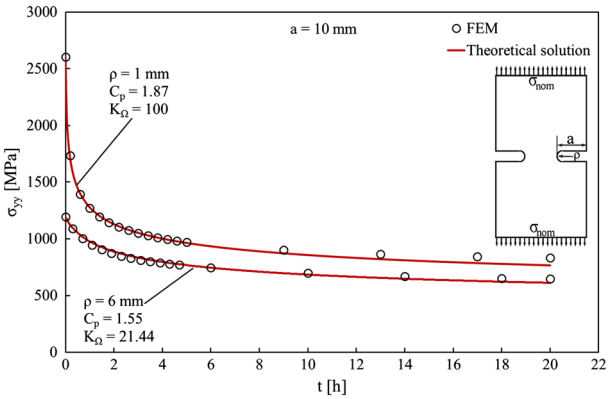

Fig. 5 Comparison between theoretical and finite element method (FEM) evolution of stresses as a function of time for U-notch geometry, $a = 10$ mm.

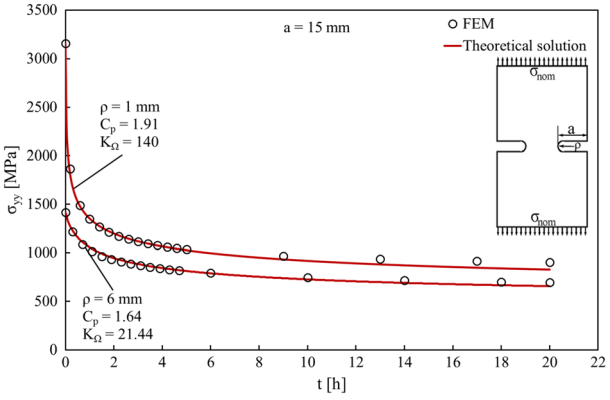

Fig. 6 Comparison between theoretical and finite element method (FEM) evolution of stresses as a function of time for U-notch geometry, $a = 15$ mm.

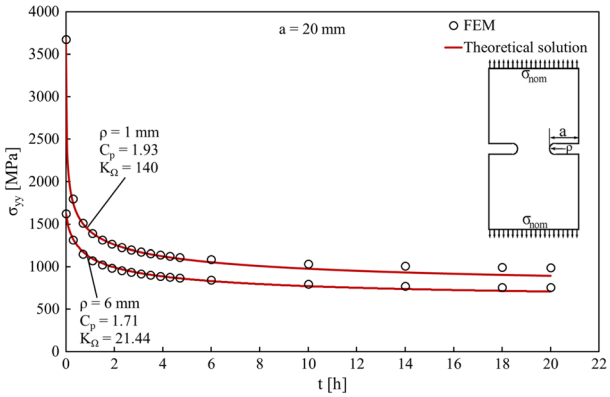

Fig. 7 Comparison between theoretical and finite element method (FEM) evolution of stresses as a function of time for U-notch geometry, $a = 20$ mm.

Examples of the new method applied to blunt V-notches: considerations and comparison between numerical and finite element analyses

The proposed new method, based on the Lazzarin–Tovo equations,[16] has been applied to a hypothetical plate weakened by lateral symmetric V-notches, under mode I loading. The notch-tip radius ρ and the opening angle 2α have been varied, while for the notch depth a, a constant value equal to 10 mm has been assumed.

Three values of the opening angle 2α have been considered: 60°, 120° and 135°. The notch-tip radius assumes for every opening angle three values: 0.5, 1 and 6 mm. Figure 8 depicts the considered geometry. The plate has a constant height, H, equal to 192 mm and a width, W, equal to 100 mm.

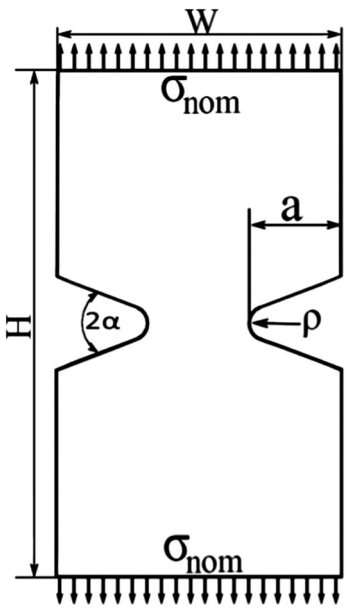

Fig. 8 Plates weakened by lateral symmetric V-notches.

The numerical results have been obtained thanks to the implementation of the new developed method and its equations in the MATLAB® software. As discussed earlier, for small tip radius the distance at which the elastic contribution is evaluated has to be larger than three times the notch radius, in order to be in the elastic field. All these values have been determined through a FE linear elastic analysis applying 345 MPa of nominal stress and are reported in Table 4, where r expresses the distance measured from the origin of the coordinates system (the so-called d in the original formulation), while $x(\rho)$ expresses the distance measured from the notch tip as a function of the notch radius.

An FE analysis has been carried out through the ANSYS code following the modelling setting summarized in the previous section. The material elastic (E, ν, σ_{ys}) and creep (n, B) properties are reported in Table 3. The creep law has been modelled as reported in Eq. (25). The procedures to simulate the creep relaxation are the same presented previously: a load has been applied instantaneously in a first load step and subsequently, in a second load step, it has been maintained constant for the desired time t. The obtained results are summarized in Figs 9–20, ordered as a function of the notch opening angle 2α for the sake of clarity.

For the sake of brevity, only few examples are reported, showing the best and worse results. In detail, Figs 9–17 depict the stress relaxation for different opening angles and notch-tip radii, while Figs 18–20 give examples of the strain evolution considering an opening angle of 120° and notch radius equal to 0.5, 1 and 6 mm, respectively. All the other cases present the same trend and are here omitted in order to not be redundant with the number of figures.

The theoretical results are in good agreement with the numerical FE values. All the stresses and strains as a function of time have been predicted with acceptable and quite limited errors.

However, from the analyses emerges a repetitive behaviour: regardless of the opening angle, the stresses of the notch radius of 0.5 mm are slightly overestimated, while the stresses of the notch radius of 6 mm are slightly

Table 4 Distance r (measured from the origin of the coordinates system) at which the elastic contribution is evaluated; x is the distance from the notch tip

ρ (mm)	$x(\rho)$	r (mm)		
		$2\alpha = 60°$	$2\alpha = 135°$	$2\alpha = 120°$
0.5	$40*\rho$	20.2	20.125	20.1
1	$18*\rho$	18.4	18.25	18.2
2	$9*\rho$	18.8	18.5	18.4
6	$3*\rho$	20.4	19.5	19.2

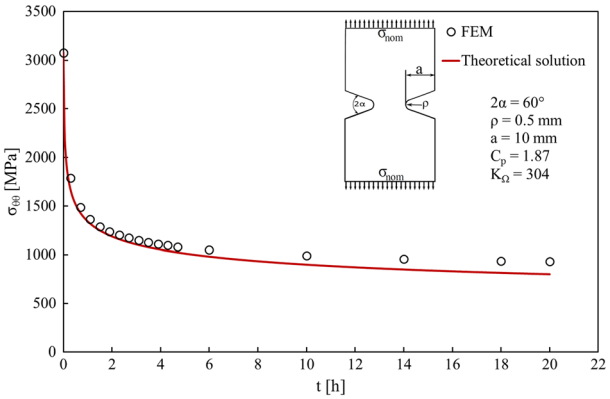

Fig. 9 Comparison between theoretical and finite element method (FEM) evolution of stresses as a function of time for V-notch geometry.

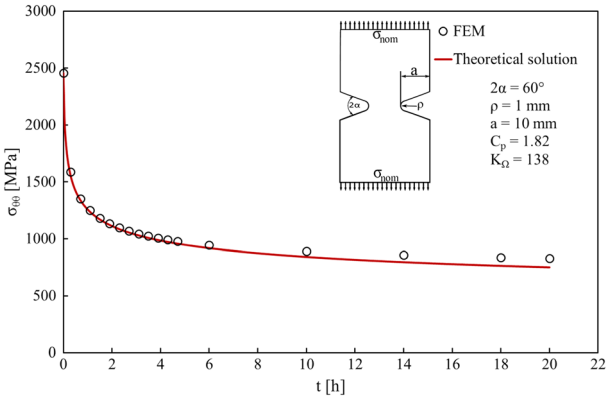

Fig. 10 Comparison between theoretical and finite element method (FEM) evolution of stresses as a function of time for V-notch geometry.

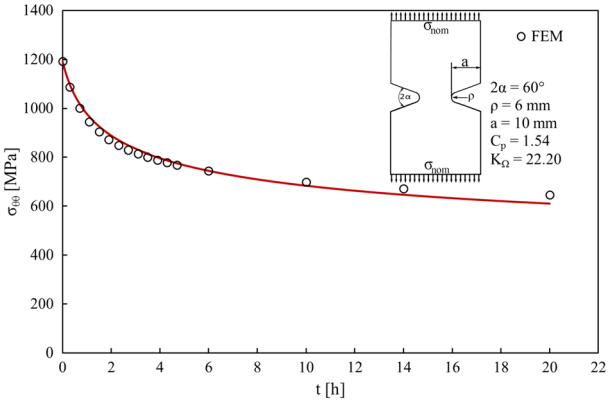

Fig. 11 Comparison between theoretical and finite element method (FEM) evolution of stresses as a function of time for V-notch geometry.

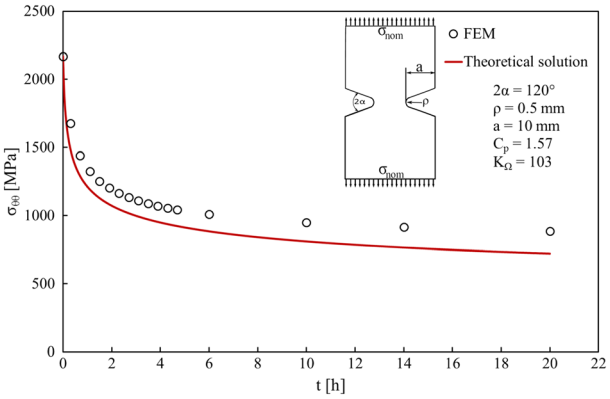

Fig. 12 Comparison between theoretical and finite element method (FEM) evolution of stresses as a function of time for V-notch geometry.

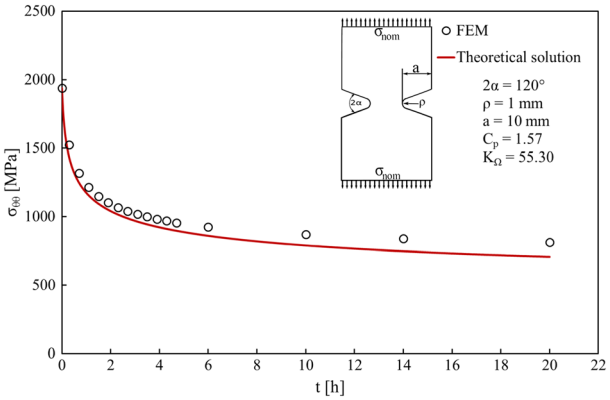

Fig. 13 Comparison between theoretical and finite element method (FEM) evolution of stresses as a function of time for V-notch geometry.

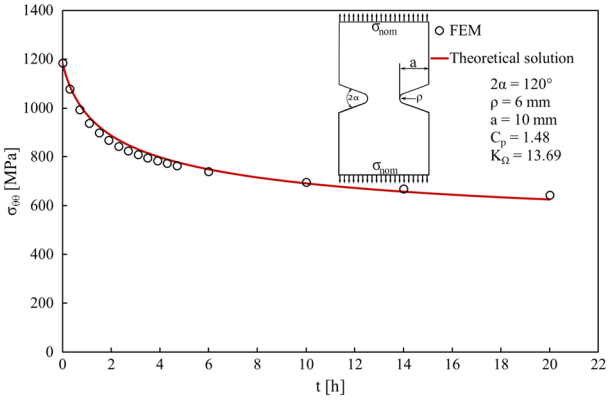

Fig. 14 Comparison between theoretical and finite element method (FEM) evolution of stresses as a function of time for V-notch geometry.

underestimated. The best solution is shown for the notch radius equal to 1 mm. Moreover, it is evident that the stresses present, after the relaxation phase, a plateau reached after almost the same time, that is, approximately 5 h, regardless of the specimen geometries. This means that the relaxation is mostly governed, as expected, by

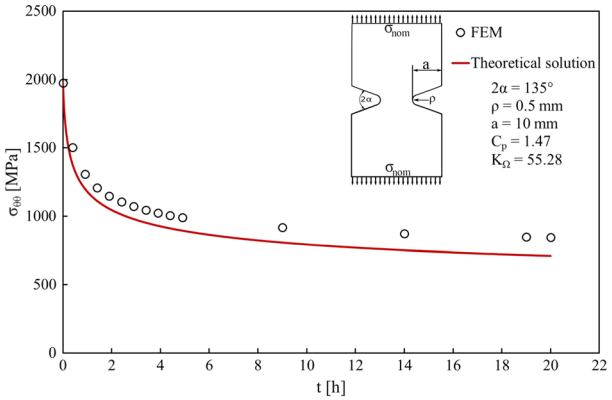

Fig. 15 Comparison between theoretical and finite element method (FEM) evolution of stresses as a function of time for V-notch geometry.

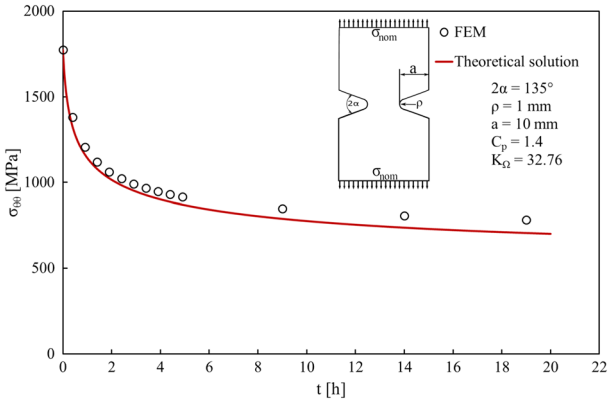

Fig. 16 Comparison between theoretical and finite element method (FEM) evolution of stresses as a function of time for V-notch geometry.

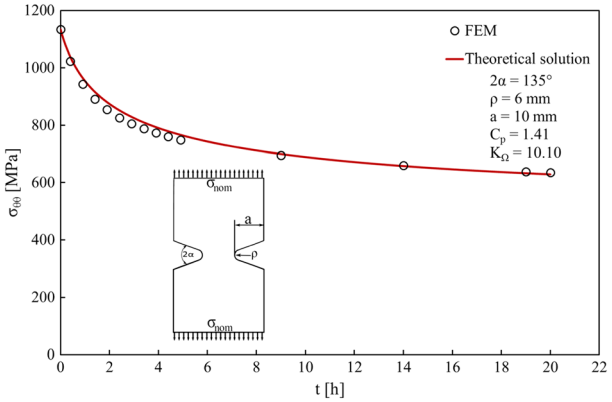

Fig. 17 Comparison between theoretical and finite element method (FEM) evolution of stresses as a function of time for V-notch geometry.

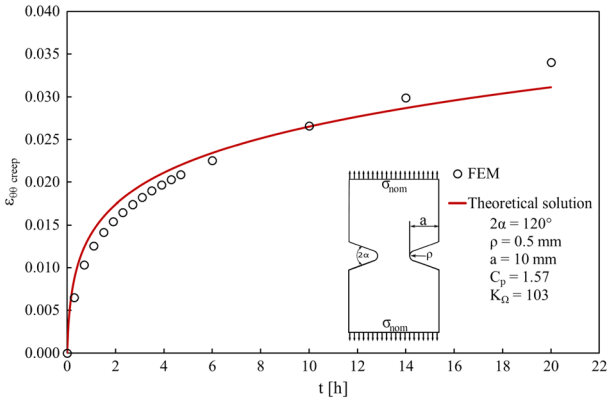

Fig. 18 Comparison between theoretical and finite element method (FEM) evolution of strains as a function of time for V-notch geometry.

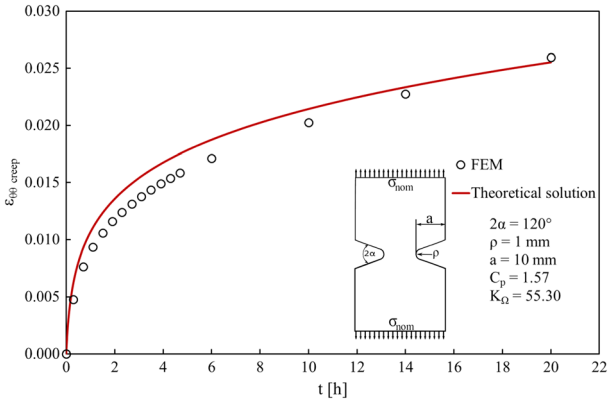

Fig. 19 Comparison between theoretical and finite element method (FEM) evolution of strains as a function of time for V-notch geometry.

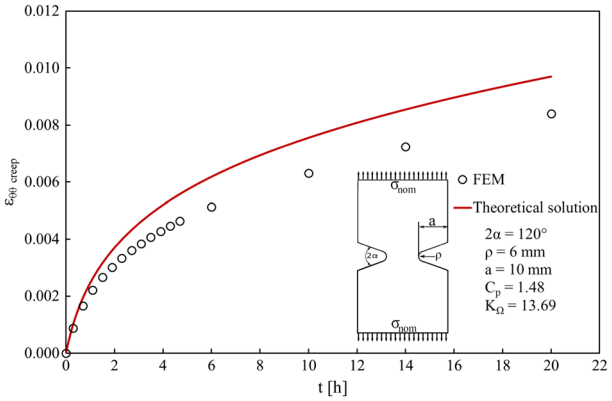

Fig. 20 Comparison between theoretical and finite element method (FEM) evolution of strains as a function of time for V-notch geometry.

the creep law, while the geometries only act on the values reached by stress and strain. Once the properties of the material is known or assumed, only one geometry must be analysed, because the trend of stress and strain and the plateau are almost the same regardless of the specimen geometries.

Considering the examples of the strain prediction depicted in Figs 18–20, from the analyses, a repetitive behaviour emerges as previously stated for the stress evolution: the best solution is obtained for the notch radius of 0.5 mm, while the error increases as the notch radius becomes bigger, with an overestimation of the strain values by the theoretical solution. The discrepancy within numerical and predicted solution can be considered acceptable for all the geometries with the exception of the last case where a notch-tip radius of 6 mm is considered. For this configuration, the strain is clearly overestimated by 20%. This error is most likely due to different approximations introduced in the theoretical formulation, such as the assumption of the elastic-perfectly plastic behaviour of the material inside the plastic zone and the employment of the Irwin's method to estimate the plastic radius. Among them, enhancement in the estimation of the plastic zone can lead to the major improvements of the strain results. However, other researchers have found bigger discrepancy within FE results and theoretical prediction when dealing with notch strains under creep condition. Just to name one example, Hatanaka *et al.*[25] studied the high-temperature creep damage caused by voids generated at grain boundary. In that paper, notched components of 2.25% Cr–1% Mo steel, whose microstructure was prepared to be characteristic of the heat-affected zone in the welded joint by heat treatments, were creep tested at 630 °C. The stress/deformation state around the notch was calculated using FEM. The strains obtained from experiment and FEM calculation were not in good agreement, showing a very high error. However, all the parameters related to the stress state (and also the minimum creep strain rate) were in good agreement comparing numerical/theoretical and experimental results.

DISCUSSION

The main advantage of the proposed method is that it permits a fast evaluation of the stresses and strains at notches under non-localized creeping condition, without the use of complex and time-consuming FE nonlinear analyses. In fact, even if the theoretical formulation seems to be complex, once the equations are implemented numerically in any commercial software, the evaluation of stress and strain is really fast and easy. The obtained stresses and strains can be used as input parameters for creep life prediction models for components subjected to mode I loading and in general on creep models based on local approaches. Moreover, the method has good potentialities to be extended to multiaxial fatigue.

It is clear that stress and strain are evaluated under non-localized creep only at the notch tip and not at some points ahead of the notch tip. The local values of stress and strain are useful when local approaches have been selected as the tool for life assessment or design. This is true not only in case of creep but, for example, also for fatigue life assessment. As well known, local approaches based on stresses and strains failed when the stress fields tend towards infinity (such as for crack or sharp notches). In these cases, the evaluation of stress and strain at some points ahead of the notch tip may be a possible way to address the problem.

Different methods are available in literature dealing with this matter, for example, the theory of critical distances or energy-based approaches such as strain energy density. These methods, even if defined for linear elastic conditions, have shown recently some good potentialities also under nonlinear conditions.

The strain energy method has been recently proposed by the authors as the characterizing parameter for high-temperature fatigue of different materials[26–32] with very good results in fatigue assessment. This parameter could be useful also to characterize creeping conditions if combined with the present model, giving the possibility to include in the analysis also sharp V-notches and cracks. In these geometries, a localized approach in terms of stress/strain is no longer suitable because of the stress concentration effect, but a strain energy density averaged over a control volume-based method[33,34] could lead to a very good solution, overcoming the problem that, at the notch tip, the stress tends towards infinity.

The theory of critical distances[35–38] has been recently applied also at high temperature, showing good capability in the fatigue strength assessment under nonlinear condition.[39]

In light of these recent and promising findings, further investigations on creep, fatigue at high temperature and their interactions are surely necessary.

With the aim to better support the reliability of the method proposed here, experimental validation and discussion on constitutive laws are also ongoing. Moreover, the estimation of the strain should be improved considering a better formulation of the plastic zone than the one proposed by Irwin and used here.

CONCLUSIONS

The present paper proposed an extension of the method presented by Nuñez and Glinka.[14] The method was proposed originally for the estimation of stress and strain at U-notches tip under non-localized creep. Non-localized (or gross) creep condition refers to situations in which the far stress field also experiences some creep and this may contribute to more intense creeping around the notch tip. In the present paper, the original work has been extended to blunt V-notches. The key to obtaining

the extension to blunt V-notches is the substitution of the Creager–Paris equations[15] with the more general Lazzarin–Tovo equations[16] that allow a unified approach to the evaluation of linear elastic stress fields in the neighbourhood of crack and notches.

The results have shown a good agreement between numerical and theoretical values. Thanks to the extension to blunt V-notches, all geometries can be easily treated with the aim of the numerical method developed.

The main results are as follows:

- The solution proposed by Nuñez and Glinka[14] presents good results for U-shaped notches. However, for small tip radii, the distance d at which the far-field contribution is evaluated has to be larger than three times the notch radius, in order to be in the elastic field;
- The distance d at which the far-field contribution is evaluated can be considered as a function of the geometry of the notch tip;
- From the analyses, it emerges a repetitive trend of the strain evolution: regardless of the opening angle, the best solution is obtained for the notch radius of 0.5 mm, while the error increases as the notch radius becomes bigger, with an overestimation by the theoretical solution of the strain values. However, even if a few cases are not in good agreement with the FEM analysis (error less than 20%), it does not affect the reliability of the procedure as shown also by other authors;
- The error found in some cases for the strain estimation is most likely due to different approximations introduced in the theoretical formulation, such as the assumption of the elastic-perfectly plastic behaviour of the material inside the plastic zone and the employment of Irwin's method to estimate the plastic radius;
- The original solution proposed by Glinka[14] cannot be directly extended to sharp V-notches. In fact, because the method is Neuber's rule based, in case of sharp notches, the peak stress tends towards infinity;
- By introducing the Lazzarin–Tovo equations, the method has been extended beyond the validity of the Creager–Paris equation, to blunt V-notches. All the results show a very good agreement within the numerical and FEM stresses;
- It is evident that the stresses present, after the relaxation phase, a plateau reached after almost the same time, that is, approximately 5 h, regardless of the specimen geometries. This means that the relaxation is mostly governed, as expected, by the creep law, while the geometries only act on the values reached by stress and strain. Once the properties of the material are known or assumed, only one geometry must be analysed, because the trend of stress and strain and the plateau are almost the same regardless of the specimen geometries. Moreover, if in addition, the peak stress is known for every geometries (thanks to K_t), all the trends can be easily reconstructed starting from a single analysis;
- The Creager–Paris equation can be derived from Lazzarin–Tovo equations. For this reason, the solution proposed in the present paper for blunt V-notches can be considered as a general solution for different notch geometries (also U-notches);
- Neglecting the far-field contribution, it can be easily derived the localized creep formulation.

REFERENCES

1 Berto, F., Campagnolo, A. and Gallo, P. (2015) Brittle failure of graphite weakened by V-notches: a review of some recent results under different loading modes. *Strength Mater.*, **47**, 488–506.
2 He, Z., Kotousov, A. and Berto, F. (2015) Effect of vertex singularities on stress intensities near plate free surfaces. *Fatigue Fract. Eng. Mater. Struct.*, **38**, 860–869.
3 Berto, F., Campagnolo, A. and Lazzarin, P. (2015) Fatigue strength of severely notched specimens made of Ti-6Al-4V under multiaxial loading. *Fatigue Fract. Eng. Mater. Struct.*, **38**, 503–517.
4 Sih, G. C. (2015) Redemption of the formalism of segmented linearity: multiscaling of non-equilibrium and non-homogeneity applied to fatigue crack growth. *Fatigue Fract. Eng. Mater. Struct.*, **38**, 621–628.
5 Tang, K. K. and Li, S. H. (2015) Interactive creep-fatigue crack growth of 2024-T3 Al sheets: selective transitional functions. *Fatigue Fract. Eng. Mater. Struct.*, **38**, 597–609.
6 Zhuang, F. K., Tu, S. T., Zhou, G. Y. and Wang, Q. Q. (2015) A small cantilever beam test for determination of creep properties of materials. *Fatigue Fract. Eng. Mater. Struct.*, **38**, 257–267.
7 Skelton, R. P. (1983) Fatigue at high temperature. *Applied Science Publishers*, **1983**.
8 Neuber, H. (1961) Theory of stress concentration for shear-strained prismatical bodies with arbitrary nonlinear stress–strain law. *J. Appl. Mech.*, **28**, 544.
9 Kubo, S. and Ohji, K. (1986) Development of simple methods for predicting plane-strain and axi-symmetric stress relaxation at notches in elastic-creep bodies. In: *Proceedings of the International Conference on Creep*. JSME, Tokyo, Japan, 1986, pp. 417–422.
10 Moftakhar, A. A., Glinka, G., Scarth, D. and Kawa, D. (1994) Multiaxial stress–strain creep analysis for notches. In: *ASTM Special Technical Publication*, Philadelphia, PA, USA. Vol. **1184**, ASTM, pp. 230–243.
11 Härkegård, G. and Sørbø, S. (1998) Applicability of Neuber's rule to the analysis of stress and strain concentration under creep conditions. *J. Eng. Mater. Technol.*, **120**, 224–229.
12 Chaudonneret, M. and Culie, J. P. (1985) Adaptation of Neuber's theory to stress concentration in viscoplasticity. *Rech. Aerosp. English Ed.*, **4**, 33–40.
13 Zhu, H., Xu, J. and Feng, M. (2011) Singular fields near a sharp V-notch for power law creep material. *Int. J. Fract.*, **168**, 159–166.
14 Nuñez, J. and Glinka, G. (2004) Analysis of non-localized creep induced strains and stresses in notches. *Eng. Fract. Mech.*, **71**, 1791–1803.

15 Creager, M. and Paris, P. (1967) Elastic field equations for blunt cracks with reference to stress corrosion cracking. *Int. J. Fract. Mech.*, **3**, 247–252.
16 Lazzarin, P. and Tovo, R. (1996) A unified approach to the evaluation of linear elastic stress fields in the neighborhood of cracks and notches. *Int. J. Fract.*, **78**, 3–19.
17 Norton, F. H. (1929) *The Creep of Steel at High Temperatures*, McGraw-Hill: New York, pp. 1929.
18 Glinka, G. (1985) Calculation of inelastic notch-tip strain–stress histories under cyclic loading. *Eng. Fract. Mech.*, **22**, 839–854.
19 Molski, K. and Glinka, G. (1981) A method of elastic–plastic stress and strain calculation at a notch root. *Mater. Sci. Eng.*, **50**, 93–100.
20 Von Mises, R. (1913) Mechanik der festen Körper im plastisch-deformablen Zustand. *J. Math. Phys.*, **1**, 582–592.
21 Irwin, G. R. (1968) Linear fracture mechanics, fracture transition, and fracture control. *Eng. Fract. Mech.*, **1**, 241–257.
22 Irwin, G. R. (1957) Analysis of stresses and strains near the end of cracking traversing a plate. *J. Appl. Mech.*, **24**, 361–364.
23 Williams, M. L. (1952) Stress singularities resulting from various boundary conditions. *J. Appl. Mech.*, **19**, 526–528.
24 Glinka, G. and Newport, A. (1987) Universal features of elastic notch-tip stress fields. *Int. J. Fatigue*, **9**, 143–150.
25 Hatanaka, K., Yahya, A. N., Nonaka, I. and Umaki, H. (1999) Initiation of high temperature creep voids in notched components. *JSME Int. J. Ser. A*, **42**, 280–287.
26 Gallo, P., Berto, F. and Lazzarin, P. (2015) High temperature fatigue tests of notched specimens made of titanium Grade 2. *Theor. Appl. Fract. Mech.*, **76**, 27–34.
27 Berto, F., Gallo, P. and Lazzarin, P. (2014) High temperature fatigue tests of un-notched and notched specimens made of 40CrMoV13.9 steel. *Mater. Des.*, **63**, 609–619.
28 Berto, F., Lazzarin, P. and Gallo, P. (2015) High temperature fatigue tests and crack growth in 40CrMoV13.9 notched components. *J. Strain Anal. Eng. Des.*, **49**, 244–256.
29 Gallo, P. and Berto, F. (2015) High temperature fatigue tests and crack growth in 40CrMoV13.9 notched components. *Frat. ed Integrita Strutt.*, **9**, 180–189.
30 Berto, F. and Gallo, P. (2015) Extension of linear elastic strain energy density approach to high temperature fatigue and a synthesis of Cu–Be alloy experimental tests. *Eng. Solid Mech.*, **3**, 111–116.
31 Berto, F., Gallo, P. and Lazzarin, P. (2014) High temperature fatigue tests of a Cu–Be alloy and synthesis in terms of linear elastic strain energy density. *Key Eng. Mater.*, **627**, 77–80.
32 Gallo P., Berto F. (2015) Influence of surface roughness on high temperature fatigue strength and cracks initiation in 40CrMoV13.9 notched components. *Theor. Appl. Fract. Mech.*, **80**, 226–234.
33 Berto, F. and Lazzarin, P. (2014) Recent developments in brittle and quasi-brittle failure assessment of engineering materials by means of local approaches. *Mater. Sci. Eng. R Reports*, **75**, 1–48.
34 Berto, F., Lazzarin, P. and Wang, C. H. (2004) Three-dimensional linear elastic distributions of stress and strain energy density ahead of V-shaped notches in plates of arbitrary thickness. *Int. J. Fract.*, **127**, 265–282.
35 Taylor, D. (1999) Geometrical effects in fatigue: a unifying theoretical model. *Int. J. Fatigue*, **21**, 413–420.
36 Taylor, W. (2000) The validation of some methods of notch fatigue analysis. *Fatigue Fract. Eng. Mater. Struct.*, **23**, 387–394.
37 Susmel, L. and Taylor, D. (2003) Fatigue design in the presence of stress concentrations. *J. Strain Anal. Eng. Des.*, **38**, 443–452.
38 Susmel, L. and Taylor, D. (2003) Two methods for predicting the multiaxial fatigue limits of sharp notches. *Fatigue Fract. Eng. Mater. Struct.*, **26**, 821–833.
39 Louks, R. and Susmel, L. (2015) The linear-elastic theory of critical distances to estimate high-cycle fatigue strength of notched metallic materials at elevated temperatures. *Fatigue Fract. Eng. Mater. Struct.*, **38**, 629–640.